Compact Objects and Binaries in Dense Star Clusters
Proceedings IAU Symposium No. 398, 2026
H. M. Lee, J. Hong & R. Spurzem, eds.
doi:10.1017/S1743921325104110

Resonant Relaxation in the Galactic Center: Multi-Component Stellar System Cases

Yoko Funato

University of Tokyo
email: funato@artcompsci.org

Abstract. We performed a series of N-body simulations of a star cluster model in our Galactic Center (GC) using realistic scale and numbers of particles. We employed two kinds of models: with and without an Intermediate Mass Black Hole (IMBH). We found that: (1) Resonant Relaxation (RR) takes place. (2) If the change in inclination of S stars driven by RR is observed, it can be a clue to estimate of the enclosed mass and object composition within apocenter of S stars. (3) If there is an IMBH, the magnitude of the change in inclination is similar to that of the RR, but may differ by a few factors. This makes it difficult to accurately estimate enclosed mass of a GC using the RR.

Keywords. S2, resonant relaxation, enclosed mass, intermediate mass black hole

1. Introduction

There is a massive Black Hole (MB) at the Galactic Center (e.g., EHT 2022). It is believed that the MBH is surrounded by stars and compact objects, although only a few dozen of stars have been observed. The observed stars are called as S stars. S stars are orbiting the black hole along their Kepler orbits. From the magnitude of observed precession of S2, the mass of MBH and the enclosed mass within S2's apocenter are estimated (GRAVITY Collaboration 2023, 2024). However, its magnitude is due to the combined effects of, at least, three factors: enclosed mass, GR and RR.

We performed a series of N-body simulations of a star cluster model in the GC using realistic scale and numbers of particles. We found that in the GC, RR takes place and it may be observed as a part of precession and change in inclination of S stars. We also show the change in inclination is due solely to RR. If its magnitude is enough large to be observed, it will be a clue to estimate of the more acurate enclosed mass and composition of objects within apocenter of S stars.

2. Model

Figure 1 shows our numerical model schematically. The SMBH with its mass $M_{\rm SMBH}$ is set to the origin. The star symbols represent individual stars. Each of them is modeled by a point-mass particle. At the initial condition, the orbit of the particle representing S2 is in the x-y plane. We adopted the mass of the SMBH is $4.3 \times 10^6 M_\odot$, the initial semi-major axis of S2, a, is 125.058 mas (1030 AU adopting the distance to the GC, R_0, as 8.2467 kpc) and its initial eccentricity is 0.884649 (GRAVITY Collaboration 2020).

The total mass of the star cluster, $M_{\rm total}$, the enclosed mass within the apocenter of S2, $M_{\rm cl}$, the number of star particles, N, are parameters which are summarized in Table 1†.

† We are performing simulations of models of wider parameter space and more runs whose results will be shown in Funato & Makino (in prep.).

© The Author(s), 2026. Published by Cambridge University Press on behalf of The International Astronomical Union. This is an Open Access article, distributed under the terms of the Creative Commons Attribution licence (https://creativecommons.org/licenses/by/4.0/), which permits unrestricted re-use, distribution and reproduction, provided the original article is properly cited.

https://doi.org/10.1017/S1743921325104110 Published online by Cambridge University Press

Table 1. Parameters of selected models and runs reported in this manuscript. mass unit: $M_\odot$. $n = 1, 5, 10$. We carried out $N_{\rm run}$ runs changing the seed for initial distribution of the star cluster in each model.

ID	$M_{\rm total}[10^4]$	$N_{\rm total}$	$M_{\rm cl}[10^4]$	m_*	$m_*/M_{\rm MBH}$	$M_{\rm IMBH}$	$N_{\rm run}$
m1-n	6.394	nk	1.2	$63.26/n$	$1.48470000/n \times 10^{-5}$	-	20
m2-n	4.682	nk	0.88	$46.39/n$	$1.08878000/n \times 10^{-5}$	-	20
m3-n	2.979	nk	0.56	$29.52/n$	$6.92860000/n \times 10^{-6}$	-	20
mi1-1	6.394	980	1.2	63.26	$1.48470000 \times 10^{-5}$	1000	20

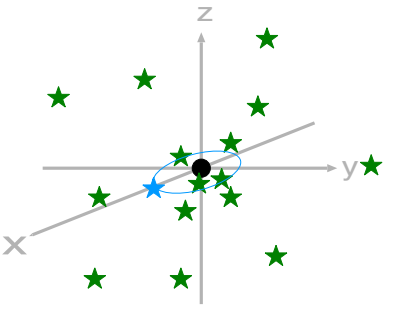


Figure 1. Schematic figure of our cluster model. As the structure of the star cluster at the initial condition, we adopted an η-model proposed by Matsubayashi et al, (2007), which is a dynamically stable stellar system model containing a massive object at its center.

3. Method

We carried out a series of direct N-body simulations using GPLUM (Ishigaki et al. 2021). GPLUM is a code developed to integrate an N-body system containing a gravitationally dominant object at its center, such as the Sun in the Solar System.

Numerical computations and analysis were carried out on PC cluster, Cray XC50 and analysis servers at the Center for Computational Astrophysics, National Astronomical Observatory of Japan.

4. Result

Here we show highlights of our work. More information will be presented in Funato & Makino (in prep.).

4.1. *precession*

Figure 2(a) shows the time evolution of argument of periaps ϕ of S2. Each curve corresponds to each run in model1-1. Figures 2(b) and 2(c) show contributions of general relativistic effect (GR) and the mean field of the star cluster (MF) to change in precession, respectively. In Figure 2(d), shown is the residual after subtracting contributions of GR and MF. Figure 2(d) shows the contribution of RR. Though change due to RR exists, to estimate its contribution from observational data is complicated because of other two effects (GR and MF).

4.2. *inclination evolution*

On the other hand, the effect of RR is clearly observed in the time evolution of inclination of S2. (It is sometimes called as Vector Resonant Relaxation (VRR)).

Figure 3(a) shows time evolution of inclination of each run of model m1-1. The change in inclination also increases/decreases linearly over time, as same as that in argument

https://doi.org/10.1017/S1743921325104110 Published online by Cambridge University Press

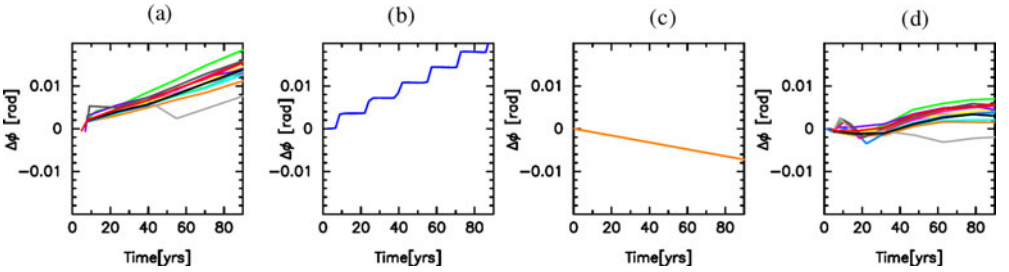


Figure 2. Change of argument of periaps. (a) observed (b) due to GR (c) due to MF (d) residual: (a)-(b)-(c).

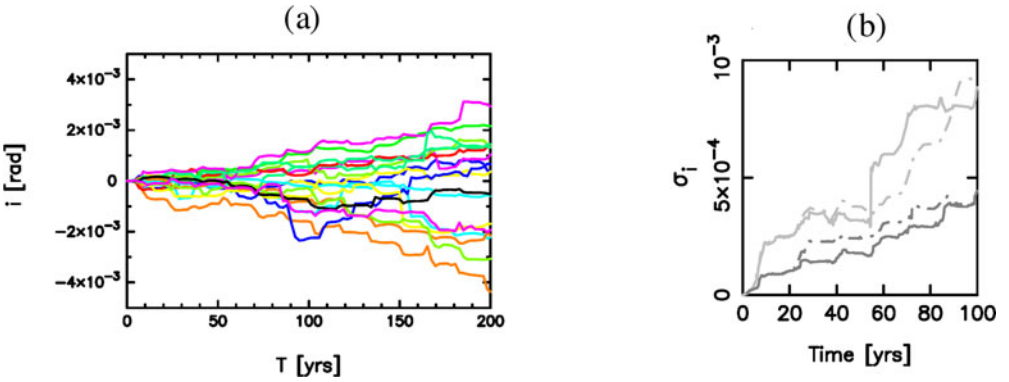


Figure 3. (a)Example of time evolution of inclination. (b)Comparison of time evolution of argument of σ_i between w and wo GR effect.

of periaps. Whether it increases or decreases depends on the bias of the initial particle distribution. For the axisymmetricity of the cluster model, there are no contribution from MF.

In figure 3(b), we compare the time evolution of inclination between in the cases with GR and without GR. The curves in figure 3(b) show the time evolution of variance σ_i. The light and dark gray curves correspond to the cases with models m1-1 and m1-5, respectively. The solid and dotted curves correspond to with and without GR, respectively. This figure shows that there is no effect of GR to the evolution of inclination. So in the following sections, we investigate the effect of RR from the point of view of evolution of inclination.

4.2.1. dependence on cluster properties

We summarize the dependence of growth rate of variance of inclination on cluster properties in Figure 4. Figure 4 shows the dependence is expressed as $\Delta\sigma_{\rm i}/P \propto M_{CL}N^{-1/2}$. This is consistent with the prediction of Rauch & Tremaine (1996).

4.2.2. Effect of Intermediate Mass Black Hole (IMBH)

Figure 5 shows that time evolution of inclination. Each curve corresponds to the result of each run in model m1-1 (a) and mi1-1 (b). Note that figure 5(a) is the same figure as figure 3(a), but the width of curves is thin except for 1 run. As shown in Figure 5(a), in Figure 5(b) each curve increases/decreases linearly over time.

https://doi.org/10.1017/S1743921325104110 Published online by Cambridge University Press

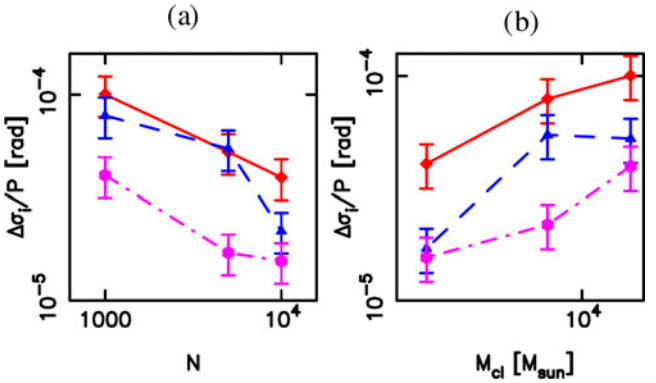


Figure 4. The growth rate of variance of change of inclination per period is plotted against $M_{\rm cl}$, which is the enclosed mass within the twice of apocenter of S2, and N. The solid, dashed and dot-dashed curves with filled-squares, filled-triangles and filled-circles (red, blue and magenta in electronical version) in Figure (a) correspond to a massive, middle and small cluster, respectively. Those in Figure (b) correspond to small, middle and large N, respectively.

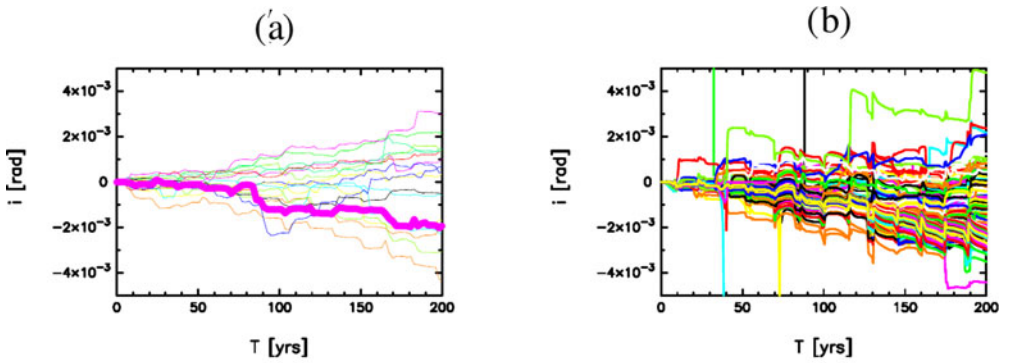


Figure 5

Figure 5. Comparison of evolution of inclination of S2 between wo(a) and w(b) an IMBH. The spikes that appear about every 12 years are numerical errors rising at pericenter passage.

The difference between the curves in Figure 5 (a) is due to the difference in the distribution of particles at the initial condition. While that between the curves in Figure 5 (b) is due to the difference in the initial position and velocity of the IMBH particle at the initial condition. The distribution of other particles is the same as that of the run corresponding to the thick curve in Figure 5 (a).

Comparing Figures 5 (a) and (b), the increasing rate of variance $\sigma_{\rm i}$ seems almost the same in both figures.

In Figure 6, we plotted time evolution of variance $\sigma_{\rm i}$ for the case with and without an IMBH. This figure shows that the time evolution of $\sigma_{\rm i}$ for the case with IMBH is in same order of that for the case without an IMBH. It is natural because RR is driven by the coherency of gravitational force from other objects. The effect of an IMBH can be equivalent to that of group of objects which is moving coherently and whose total mass is as same as that of the IMBH. But as shown in Figure 6, there is a difference of about a few times. At this point, the cause of this discrepancy is still unclear. It will be investigated in our future work.

https://doi.org/10.1017/S1743921325104110 Published online by Cambridge University Press

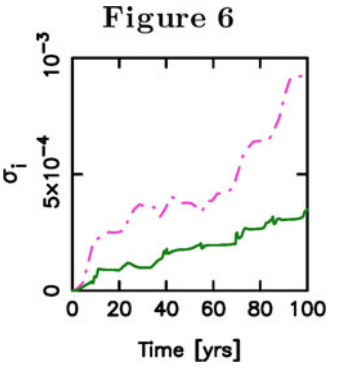


Figure 6. Time evolution of variance $\sigma_{\rm i}$ of inclination evolution. solid, dark (dark green in electronical version): with IMBH, dot-dashed, light (purple in electronical version): without IMBH.

5. Discussion

Our results suggest that for a population of equal-mass objects, the enclosed mass and N can be estimated from the evolution of the orbital inclinations of several S stars with similar apocenter distances. If the objects have a mass distribution, we need to be more careful. Even a single IMBH can have the same impact as a factor of difference in N or $M_{\rm cl}$. It may be useful to consider the presence and mass of an IMBH with a different perspective (e.g., Gualandris & Merritt 2009).

References

EHT Collaboration, 2022, ApJ*Letter*, 930, L12.
Funato, Y., & Makino, J., *in prep.*
GRAVITY Collaboration, 2020, A&A, 636, L5.
GRAVITY Collaboration, 2023, A&A, 672, A63.
GRAVITY Collaboration, 2024, A&A, 692, A242.
Gualandris, A. & Merritt, D., 2009, ApJ, 705, 361.
Ishigaki, Y., Kominami, J., Makino, J., Fujimoto, M., & Iwasawa, M., 2021, PASJ, 73, 660.
Matsubayashi, T., Makino, J., & Ebisuzaki, T., 2007, ApJ, 656, 879.
Rauch, K. P., & Tremaine, S., 1996, New Astronomy, 1, 140.

https://doi.org/10.1017/S1743921325104110 Published online by Cambridge University Press